ELSEVIER

Precision Engineering
Journal of the International Societies for Precision Engineering and Nanotechnology
25 (2001) 107–113

PRECISION ENGINEERING

Micromilling of metal alloys with focused ion beam–fabricated tools

David P. Adams[a,*], Michael J. Vasile[b], Gilbert Benavides[a], Ann N. Campbell[a]

[a]*Sandia National Laboratories, Albuquerque, NM 87185, USA*
[b]*Institute for Micromanufacturing, Louisiana Tech University, Ruston, LA 71272, USA*

Received 28 March 2000; accepted 6 September 2000

Abstract

This work combines focused ion beam sputtering and ultra-precision machining as a first step in fabricating metal alloy microcomponents. Micro-end mills having ~25 μm diameters are made by sputtering cobalt M42 high-speed steel and C2 micrograin tungsten carbide tool blanks. A 20 keV focused gallium ion beam is used to define a number of cutting edges and tool end clearance. Cutting edge radii of curvature are less than or equal to 0.1 μm. Micro-end mill tools having 2, 4 and 5 cutting edges successfully machine millimeter long trenches in 6061-T4 aluminum, brass, 4340 steel and polymethyl methacrylate. Machined trench widths are approximately equal to the tool diameters, and surface roughnesses (R_a) at the bottom of micromachined features are ~200 nm. Microtools are robust and operate for more than 6 h without fracture. Results from ultra-precision machining aluminum alloy at feed rates as high as 50 mm/minute and an axial depth of 1.0 μm are included. © 2001 Elsevier Science Inc. All rights reserved.

Keywords: Micromilling; Microtools; Ultra-precision machining

1. Introduction

Alternative microfabrication techniques [1] that complement or improve upon processes such as electro-discharge machining (EDM) and pulsed laser drilling are being explored to meet the demands of manufacturing. Additional techniques are required to enhance prototyping and production of microcomponents and micromechanical devices. In particular, there is a desire to fabricate complex features in a diverse set of workpieces or substrates. This includes creating high depth/width aspect ratio holes, curved surfaces and rectilinear features in materials other than those commonly used in the semiconductor industry. Future microfabrication will involve various metal alloys, ceramics and polymers.

Ultra-precision machining is attractive for microfabrication of different materials. The advantages of ultra-precision techniques include accurate machining of complex features, such as curvilinear shapes, and the ability to work with a variety of workpiece geometries. Recent studies also demonstrate methods for fabricating micron size features [2–4]. For example, conventional machining techniques such as lathe turning and EDM have been used to create 10 μm diameter shafts [5] and 200 μm wide rotors [6,7], respectively. In general, control over small feature size is made possible by computer numerically controlled (CNC) ultra-precision machines. These instruments have 5-nm positional accuracy in different directions and specially designed tool holders that minimize error. CNC ultra-precision machines have been used to create microfeatures while maintaining sub-μm tolerances over a span of millimeters [4].

Micromilling is an additional ultra-precision technique that shows promise of machining features down to micron length scales. The smallest commercially available milling tools [8] are ~50 μm in diameter, but research continues to fabricate and test smaller tools. Recently, a few groups [9–12] have demonstrated techniques for fabricating micromilling tools from steels and carbides. For example, mechanical grinding was used to make single edge, metal micro-end mill tools with cutting diameters of ~ 45–100 μm [9]. These tools successfully machine small grooves in brass and stainless steel workpieces; however, tool geometry could be controlled by the grinding process only to within ± 5 μm [9]. In addition, other researchers [10] have demonstrated 22 μm diameter micro-end mills shaped by focused ion beams. These tools were used to machine PMMA workpieces. Additional research with these tools fabricates thin films into X-ray lithography masks [11].

Despite these efforts, there is a need for improved techniques that controllably and reproducibly fabricate complex

* Corresponding author. Tel.: +1-505-844-8317; fax: +1-505-844-2754.
E-mail address: dpadams@sandia.gov (D.P. Adams).

0141-6359/01/$ – see front matter © 2001 Elsevier Science Inc. All rights reserved.
PII: S0141-6359(00)00064-7

cutting tools having diameters less than 100 μm. In present work, we use focused ion beam (FIB) sputtering to shape a variety of micro-end mill tools. FIB sputtering is used to fabricate tools, because this technique affords precise control over feature size, permits a variety of tool geometries and establishes sharp cutting edges. A focused ion beam is typically less than 0.5 μm in diameter, allowing for small features with sub-μm tolerances [13,14]. Commercial FIB systems provide 50 nm spot sizes with nA beam currents. Also, these systems can position tools with sub-μm accuracy, and a few can rotate samples over a large range of angles [15]. Therefore, multiple nonplanar facets [15,16] can be created to establish tool clearance, rake or taper. FIB sputtering applied to tool fabrication is well controlled due to precise beam positioning and dose allocation. Ion sources, focusing optics and beam deflectors are extremely stable over hundreds of hours. Microtool fabrication is reproducible, because ion sputtering is a relatively 'stress-free' process. Compared with techniques such as mechanical grinding, there is less force imposed on a tool that may lead to end mill fracture during fabrication.

In current work, the precision of focused ion beam sputtering is combined with ultra-precision milling to determine if metal alloys can be mechanically machined at a high rate while maintaining extremely small tolerances. Precise fabrication of microtools allows for a meaningful comparison of tool diameter and micromachined feature width for different machining parameters.

2. Experimental

Micro-end mill tools are fabricated in a 'home-built' focused ion beam system, described in detail elsewhere [17]. It consists of a liquid metal ion source, beam deflectors, sample stage, and channelplate detector for secondary electron imaging. The ion gun produces a 20 keV beam of Ga^+ ions with a Gaussian intensity distribution and a full-width at half-maximum diameter of 0.4 μm. Currents are typically 2 nA in a Faraday cup giving a current density of $\sim$ 1.5 A/cm$^{2.}$ In practice, an operator outlines a desired shape on a tool image, and an octupole deflection system steers the beam over targeted areas with sub-μm resolution. A stage positions samples with 1 μm absolute accuracy and provides for sample rotation with a minimum step size of 0.37^o per pulse. The Ga^+ source chamber is ion pumped and has a pressure of 10^{-9} Torr. The target chamber uses an oil diffusion pump to maintain a pressure of 10^{-8} Torr during sputtering. A small aperture separates the two chambers for efficient differential pumping.

Tool blanks are purchased from National Jet, Inc. and are made of materials commonly used for cutting tools, including cobalt M42 high-speed steel or C2 micrograin tungsten carbide. Tool shanks are 1.02 mm in diameter and are brazed into a centerless ground mandrel. One end of each shank is tapered by diamond grinding and polished; this end has a nominal 25 μm diameter and is cylindrical over a length of 90 μm.

Two high precision milling machines are used to test focused ion beam-fabricated microtools and to develop machining procedures. This includes a Boston Digital mill and a modified National Jet 7 M milling machine [18]. The Boston Digital apparatus has 1.0 μm resolution in the plane of the workpiece (x and y) and 0.5 μm depth resolution. Tools are held in a collet to minimize error. The National Jet 7 M instrument has a 1,500 kg granite machine base for vibrational and thermal stability, and all axes have air bearings. In addition, the x and y motions of the work table employ laser interferometry with a commanded resolution of 1.25 nm, and the z motion has linear encoder positional control with a resolution of 20 nm. All travel ranges are 150 mm. The micromilling head consists of a specially designed v-block bearing arrangement having four spherically convex diamonds. Tools rotate about an axis dictated by the contact positions of the four diamond surfaces on the tool mandrel resulting in a cumulative radial error less than 1 μm. The small error is attributed to variations in tool mandrel surface roughness. All micromachining tests involve a lubricant unless specified. Workpieces are flushed continuously during micromilling with a water-based, sulfur free liquid (Blasser 4000). All milling operations, including registry, are monitored with an optical microscope and CCD camera. Workpieces are cleaned with isopropyl alcohol after micromachining. However, in this study burrs are not removed by mechanical or electrochemical polishing.

Scanning electron microscopy (SEM) and optical interferometry are used to analyze microtools and machined workpieces. A calibrated JEOL 6300V scanning electron microscope is used to measure tool diameter, tool edge radius of curvature, trench widths and taper angles. This instrument is calibrated to a NIST/NBS standard (reference # 484 c) and shows less than 2% error for different working distances (i.e., bottom of pole piece to sample surface). An overall accuracy of 95% or better is estimated for dimensions measured by SEM. Trench widths are measured from SEM images that view normal to the plane of a workpiece. Additional images that show perspective views are not used for measurement. PMMA samples are coated with $\sim$ 20 nm of Au/Pt to prevent charging in the SEM. A calibrated WYKO (RST^+) white light optical interferometric roughness step tester determines the roughness in the bottom of machined trenches. Several regions within the bottom of each micromachined trench are probed to obtain an accurate measurement of surface roughness both laterally and longitudinally. A typical measured region is 100 μm long. PMMA samples coated with 20 nm of Au/Pt have a reflective surface for inspection. The step height standard for the roughness step tester is a 23.33 μm metal film (VLSI Standards, Inc.). The phase shift interference resolution of the RST^+ is 0.3 nm.

3. Tool fabrication

A micro-end mill is made from a polished tool blank by ion sputtering a number of nonplanar facets as shown in Figure 1.

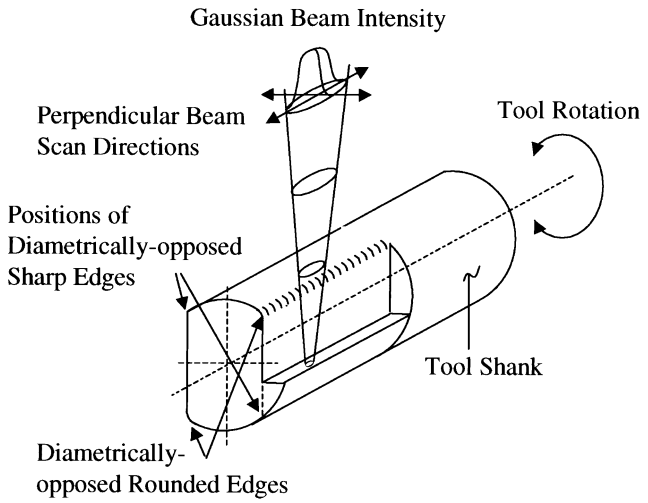

Fig. 1. Ion source/sample geometry used for fabricating micro-end mills. Schematic shows tool end.

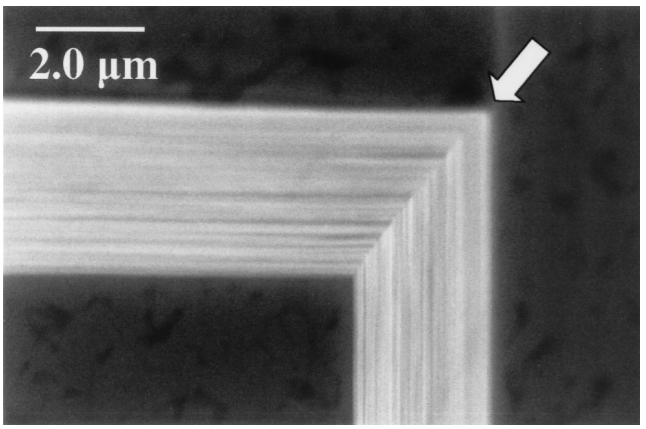

Fig. 2. Sharp cutting edge of a four-side, tungsten carbide micro-end mill tool. Edge shown is the intersection of two focused ion beam sputtered facets.

The end of a tool blank is first bombarded to remove approximately 5 μm from the 90 μm long, ~25 μm diameter cylindrical portion. This creates a polished facet with a normal direction oriented 7° with respect to the tool axis. This tool-end facet is intended to provide clearance for chip removal during mechanical milling. After modifying the tool end, the ion beam is directed over areas approximately 3 μm by 50 μm to create chip-cutting facets. With the FIB stage and tool fixed, the gallium beam impinges normal to a plane containing the tool axis, but tangential to the tool circumference. This ion-solid geometry is chosen, because it produces one extremely sharp edge per facet. The sputtered facet edge closest to the ion source is rounded having a radius of curvature, R_c, on the order of 1.0 μm. This rounding is due to the part of the Gaussian beam intensity that extends outside the user-defined pattern boundary. However, continued ion sputtering with this particular geometry makes a sharp edge, $R_c \leq 0.1$ μm, on the facet side furthest from the ion source. A sharp edge is produced, because the ion beam has a truncated intensity distribution due to shadowing by the tool facet. For this study, we designate the sharper facet edges as cutting edges. Figure 2 shows evidence of a sub-μm radius of curvature along a cutting edge. The SEM image is taken near parallel to the tool axis.

Numerous facets and sharp facet edges can be formed by using a sequence of tool rotation and sputter removal steps. The number and position of facets on a micro-end mill uniquely determine the properties of a tool, such as clearance for removing a chip and tool rotation direction for milling. Figure 3 shows micro-end mills having 2, 4 and 6 cutting facets made by focused ion beam sputtering. The tool in Figure 3.a. has two cutting facets and two diametrically opposed sharp edges. Also, this micro-end mill has a tool-end clearance facet. The tool shown in Figure 3.c. has six cutting facets and clearance behind each of the five cutting edges, since almost the entire circumference is sputtered. In this study six-facet end mill tools are made with 4, 5 or 6 sharp edges by selecting a particular stage rotation sequence between sputter steps. Independent of the number of cutting edges, the placement of facets by FIB sputtering determines tool rotation direction for milling operations. Micro-end mills have been made so that sharp facet edges cut while rotating the tool clockwise or counter-clockwise. Note, only tools made for a clockwise rotation (looking down on a workpiece) are tested in this study.

Microtools are fabricated in 2–3 h depending on micro-end mill design and tool material. In general, a tool having a large number of facets is fabricated in a relatively short time, because less material is removed. For example, the time required to make the six-facet tool shown in Figure 3.c. is less than the time needed for the other tools shown. Also, the fabrication time depends on tool material, since sputter rate is a function of the target mass. In the present work, the sputter rate for tungsten carbide is quantified by bombarding polished wafers of identical C2-grade material with a fixed gallium dose equal to 1.0×10^{19} ions/cm^2 (i = 2.8 nA) at 20keV. Areas 20 μm x 20 μm are sputtered to a small depth in order to avoid re-deposition, using a 72 μsec pixel dwell time, a 0.19 μm pixel spacing and a 0.86 sec refresh time. A single near-normal angle of incidence is used for this control experiment. Afterwards, a portion of the feature is cross-sectioned with the gallium beam, and the depth is measured away from the feature edges. Average depth is measured by tilting the sample to a known angle in the scanning electron microscope and taking several measurements along the feature bottom boundary. Using the sputtered volume, an average rate of removal is calculated for C2 carbide equal to 0.76 μm^3/sec.

When using FIB sputtering to fabricate microtools, it is also important to note that each facet forms an angle of ~ 7° with respect to the incident ion beam direction. This occurs because of minimal sputter yield at incidence angles greater than 83° with respect to the surface normal. [19] Ions impinging on a surface at near-glancing angles most often reflect without displacing atoms from lattice sites. Note, tools can be aligned with respect to the ion beam direction to compensate for this sputter-induced angle. Rotation of a tool to a slightly different orien-

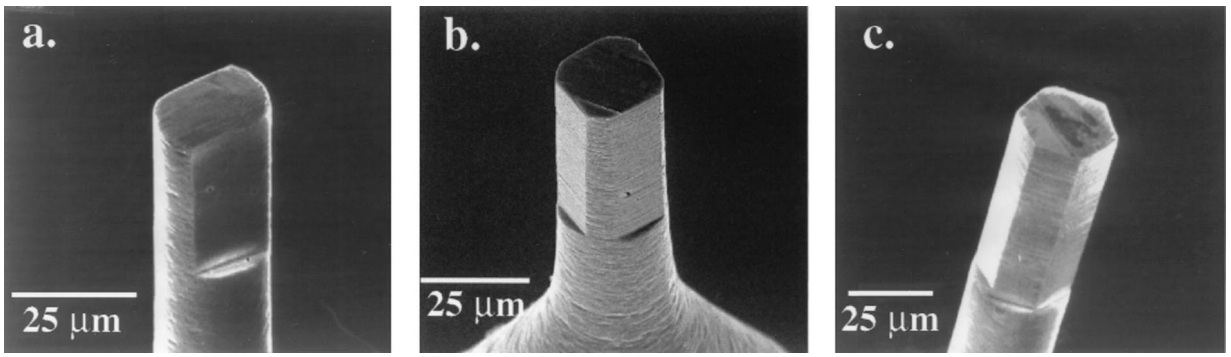

Fig 3. Micro-end mills made by focused ion beam sputtering having 2 (a), 4 (b), and 5 (c) cutting edges. Scanning electron micrographs.

tation prior to sputtering of individual facets changes the facet normal direction as desired.

4. Micromilling

4.1. Machining at feed rates of 2–3 mm/minute

Micro-end mill tools are tested by milling materials having different degrees of machinability. Initial tests of micro-end mills involve machining at low feed rates, 2 or 3 mm/minute, with an axial depth per pass ≥ 0.5 μm. These depths/pass are chosen, because a microtool 'appears' sharp when compared to the cutting action, i.e., the tool edge R_c is less than the thickness removed. Microtools are rotated clockwise in this study so that sharp facet edges cut a workpiece.

FIB-fabricated microtools successfully machine trenches in PMMA, 6061-T4 aluminum, brass and 4340 steel [20] at low feed rates. For all tests except for one, 15–25 μm deep trenches are cut several millimeters in length as commanded. As summarized in Table 1, the surface roughness (R_a) of trenches machined at low feed rates is small, ~200 nm or less. These values are averages taken from several areas within a given trench and account for both transverse and longitudinal milling directions. In addition, all trenches milled in PMMA, Al alloy and 4340 steel have nearly vertical sidewalls. Near-vertical sidewalls are present on both sides of micromachined trenches as demonstrated in 6061 Al (Figure 4.b.). Electron microscopy shows a slight taper of ~1–2° from vertical. SEM shows that micromachined trench widths are similar to the intended sizes (i.e., tool diameters). Experiments with the Boston Digital apparatus produce trench widths that are ~2 μm larger than the tool diameters. Close matching is found for the different tool designs and workpiece materials. The small deviation from the intended width is attributed to the radial error of the tool and spindle. The combination of tool form error and spindle motion radial error is measured to be 2 μm or less prior to each machining test. Error is probed approximately 2 mm from the end of the mandrel closest to the tool shank using a test indicator. Additional milling tests with the modified National Jet apparatus at large axial depths of cut and rotation speeds to 20,000 rpm produce similar matching (see tests outlined in Table 2). Trenches milled in PMMA are limited at 2 μm larger than the tool diameter. With the National Jet instrument, a tool is held in a v-block bearing assembly that is specially designed to minimize radial error beyond the variations in surface roughness of the tool mandrel. Therefore, we expect that the differences between micro-end mill diameter and trench width result from the eccentricity of tool cutting edges or possible tool vibration. In general, tests with both milling instruments produce trench widths that are uniform over several millimeters. Figure 5 shows a trench milled in

Table 1.
Machining parameters and results from micromilling different materials at a feed rate of 2 or 3 mm/minute. Depths per pass are equal to 0.5 or 1.0 μm. Boston Digital milling machine is used.

Tool #, #Cutting edges Tool Material	Tool Diameter (μm)	Workpiece Material	Rotation Speed, (rpm)	Feed Rate, (mm/min)	Depth Per pass, (μm)	Mean Trench Width, Standard Deviation (μm)	Roughness, Trench Bottom R_a (nm)
Q2, 4, HSS	24.0	PMMA	18,000	2.0	0.5	26.2, 1.5	93
H4, 4, HSS	26.2	A1 6061-T4	10,000	2.0	1.0	28.2, 1.1	92
B2, 2 HSS[†]	23.6	A1 6061-T4	18,000	2.0	0.5	30.0, 2.0	458
B3, 2, WC	21.7	A1 6061-T4	18,000	3.0	1.0	23.0, 1.1	117
H6, 5, HSS	25.0	Brass	10,000	2.0	1.0	28.8, 0.7	139
Q6, 4, WC	22.5	4340 Steel	18,000	3.0	1.0	23.5, 1.0	162

Tool # Code: 1st letter designates overall shape; H = Hex-tool (6 facets); B = Bi-tool (2 facets); Q = Quad-tool (4 facets)
Tool Material Code: HSS = High Speed Steel; WC = tungsten carbide
[†]*No lubricant used during machining. Only 22 passes completed.*

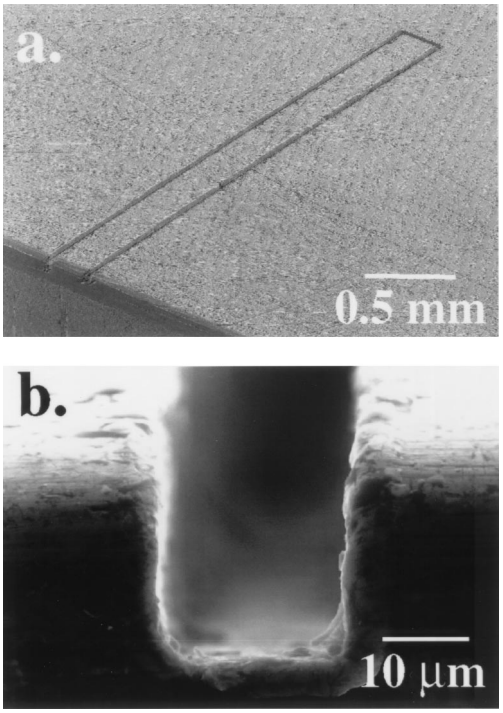

Fig 4. Al 6061 alloy machined using a two-edge micro-end mill. Scanning electron micrographs include a perspective view of an entire trench (a) and an end-on view from the edge of the workpiece (b).

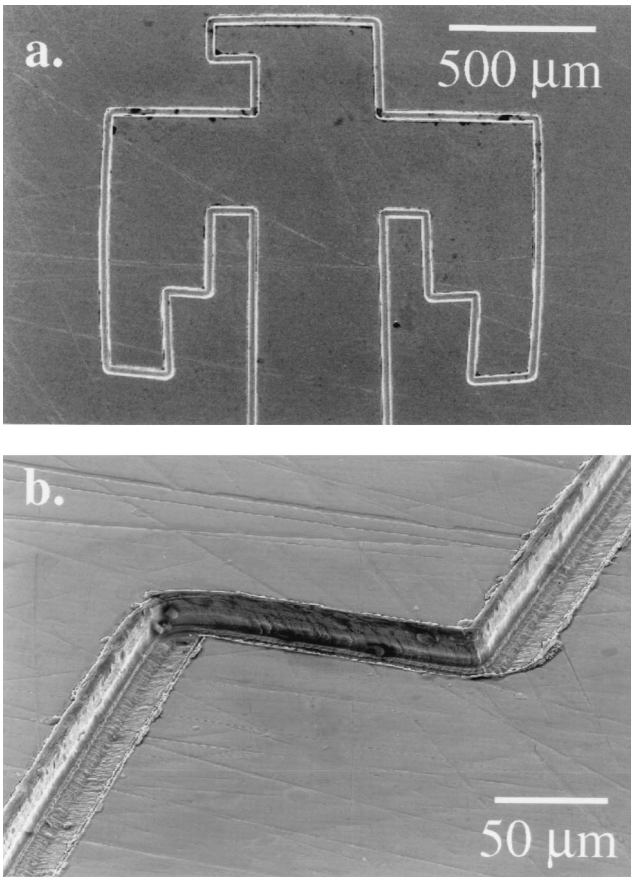

Fig. 5. Brass machined with micro-end mill tool having five cutting edges. Plan-view scanning electron micrograph is shown in (a), and a higher magnification, perspective view is shown in (b).

brass with the Boston Digital apparatus having a total length of 10 mm and a width of 28.8 μm. This feature requires 25 passes for completion and demonstrates the positioning repeatability of ultra-precision milling machines. Note the curved portions of the micromachined trench, as seen in Figure 5.a., are part of the intended design and are not image artifacts.

The experiments listed in Tables 1 and 2 show a single test that results in a significantly larger trench width and surface roughness. This is highlighted in Table 1 and involved tool 'B2′, a two facet high speed steel micro-end mill. Machining 6061 aluminum at a feed rate of 2 mm/minute without a lubricant produces a trench width approximately 6.4 μm larger than the tool diameter. Also, the roughness of the trench bottom is measured using optical interferometry to be ~458 nm. It is expected that the lack of a lubricant is responsible for the poor characteristics of this micromachined feature. Note, this ultra-precision machining test resulted in microtool fracture, with breakage occurring during the twenty-second pass. It is estimated that tool B2 is rotated 3.4×10^6 times while in contact with the workpiece prior to fracture. Approximately 6.0×10^6 μm^3 of material is removed.

There are several indications that microtools cut chips rather than remove material by burnishing. In separate experiments on PMMA and 6061 Al, the lubricant is turned off and the workpiece is blown dry for brief amounts of time to observe cutting through an optical microscope. Repeatedly there is evidence of small chips being ejected from the vicinity of a moving tool. Evidence of cutting is also found after machining PMMA

Table 2.
Machining parameters and results from micromilling PMMA using depths per pass equal to 2.5 and 5.0 μm. Modified National Jet apparatus is used.

Tool #, # Cutting edges Tool Material	Tool Diameter (μm)	Workpiece Material	Rotation Speed, (rpm)	Feed Rate, (mm/min)	Depth Per pass, (μm)	Mean Trench Width Standard Deviation (μm)	Roughness, Trench Bottom R_a (nm)
Q11, 4 HSS	28.0	PMMA	20,000	2.0	5.0	27.6, 1.4	180
Q11, 4 HSS	28.0	PMMA	20,000	2.0	2.5	30.6, 1.7	195
Q11, 4 HSS	28.0	PMMA	18,000	2.0	2.5	29.1, 2.8	190

Tool # Code: 1st letter designates overall shape; Q = Quad-tool (4 facets)
Tool Material Code: HSS = High Speed Steel

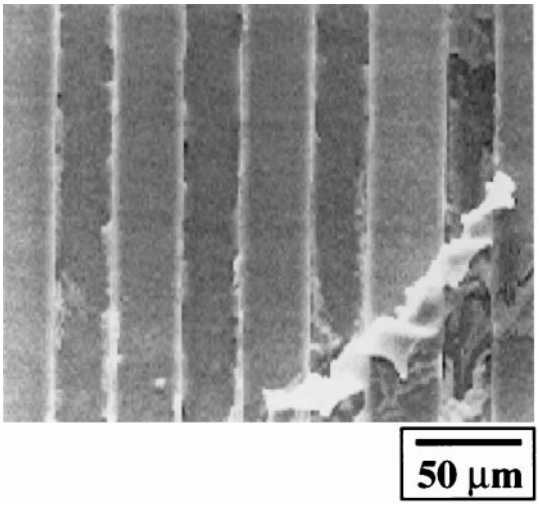

Fig. 6. Four parallel grooves milled in PMMA at 20,000 rpm with a 2mm/minute feed rate. Micrograph is taken prior to cleaning workpiece.

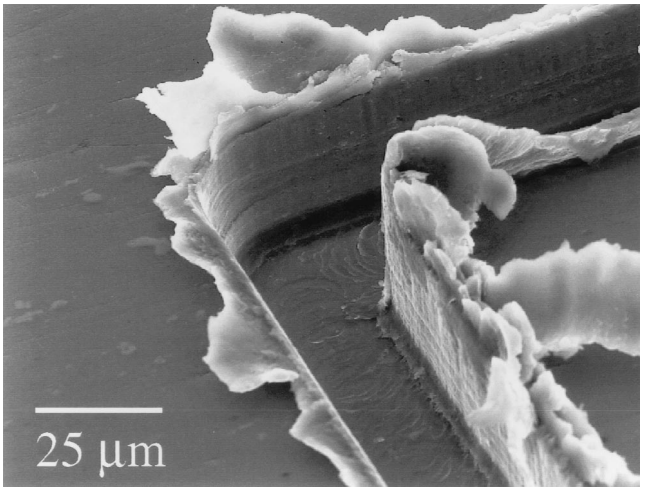

Fig 7. Scanning electron micrograph of Al 6061 machined at a feed rate of 10 mm/minute.

workpieces. Figure 6 shows the terminal section of four parallel grooves milled in PMMA at 20,000 rpm with 2.5 and 5.0 μm axial depths per cut. The curled piece of debris near the base of groove #2 indicates that PMMA is removed by cutting chips. After rinsing workpieces, trenches are inspected with SEM to determine the morphology of the bottom surface. In all cases, tool-cutting marks are revealed. Marks are found in micromachined brass, PMMA, Al alloy and steel. Figure 5.b. shows an example of tool cutting marks in brass.

4.2. Machining at feed rates of 3–50 mm/minute

Additional ultra-precision machining experiments are used to evaluate microtool performance for increased chip load rates. These milling tests involve constant table feed rates of 3, 10, 25 and 50 mm/minute, and again a tool is rotated clockwise (looking down on the workpiece) so that sharp facet edges cut. A rotation speed of 18,000 rpm is used for each test, and the axial depth per pass is equal to 1.0 μm. For each feed rate, a single two-facet microtool successfully mills 25 μm deep, 7 mm long trenches in 6061-T4 Al. The tool is made of C2 tungsten carbide and has a diameter of 21.7 μm.

As described in Table 3, micromilled trench widths are approximately the same size as the tool diameter. Average trench widths range from 22.0 to 23.1 μm. The standard deviation taken from these measurements is also included in the table. In addition, surface roughness measured in the bottom of milled trenches is approximately 200 nm or less, and there is no degradation with increased table feed rate. Figure 7 shows a portion of a trench milled in Al alloy that demonstrates typical characteristics. This particular trench is milled at a feed rate of 10 mm/minute. The sidewalls of this and other micromachined trenches are nearly vertical, and the roughness in the bottom is characterized by tool cutting marks. Chips are located around the top edge of the trench shown; this debris is not easily removed with a solvent rinse. Recent work by Schaller et al. [9] and others demonstrates techniques for chip removal/polishing that should be applicable at this smaller scale. In summary, micromilling tests at higher feed rates suggest that FIB-fabricated microtools mill metal alloys without significant tool dulling. Repeated testing indicates that FIB-fabricated tools are robust despite their small size and 'apparent' delicate nature. The two-facet microtool, labeled 'B3′ in Table 3, milled 6061 Al for over 6 h without tool fracture. At a feed rate of 50 mm/minute, aluminum alloy is machined at 18,740 μm^3/sec.

Table 3.
Machining parameters and results from micromilling A1 6061-T4 at different feed rates including 3, 10, 25 and 50 mm/minute. For these tests, the Boston Digital milling machine is used.

Tool #, # Cutting edges, Tool Material	Tool Diameter (μm)	Workpiece Material	Rotation Speed, (rpm)	Feed Rate, (mm/min)	Depth per pass, (μm)	Mean Trench Width, Standard Deviation (μm)	Roughness, Trench Bottom R_a (nm)
B3, 2, WC	21.7	A1 6061-T4	18,000	*3.0*	1.0	23.0, 1.1	117
B3, 2, WC	21.7	Al 6061-T4	18,000	*10.0*	1.0	22.0, 0.6	83
B3, 2, WC	21.7	A1 6061-T4	18,000	*25.0*	1.0	23.1, 0.6	82
B3, 2, WC	21.7	A1 6061-T4	18,000	*50*	1.0	22.5, 0.5	102

Tool # Code: 1st letter designates overall shape; B = Bi-tool (2 facets)
Tool Material Code: WC = tunsten carbide

5. Conclusions and future work

In conclusion, this work demonstrates a technique for fabricating a diverse set of materials at the microscale. Sharp micro-end mill tools made by focused ion beam sputtering machine ~ 25 μm wide features in different metal alloys. Accurate placement of facets on tools and a proper stage rotation sequence between ion sputter steps is used to make micro-end mills of different geometries. This includes creation of well-aligned, nonplanar, cutting and tool-end clearance facets. Ultra-precision machining is used to fabricate trenches that are several millimeters long. Trenches have nearly vertical sidewalls and small bottom surface roughness. A good matching of tool diameter to trench width is found for all materials tested including PMMA, 6061 Al, 4340 steel and brass. This includes machining at table feed rates up to 50 mm/minute.

The technique used for making micro-end mills is capable of fabricating even smaller tools. Beam sizes for the FIB system are 0.4 μm, and positioning resolution is less than 1 μm. Tools made to smaller dimensions must, of course, have suitable microstructures that provide strength and toughness necessary for cutting. Single crystal diamond tools will be attempted in future work. It is expected that FIB sputtering can also be used to make more complex micro-cutting tools and is not limited to micro-end mills. For example, high-precision threading and grooving tools for lathe machining of nonplanar workpieces are feasible. In the immediate future, FIB sputter fabrication of microtools will involve creation of a number of nonplanar facets but not curved surfaces, such as that found on spiral flutes. Although fabrication of curved surfaces remains a difficult task complicated by the sputter yield dependence on incidence angle, recent progress [21] has been made toward 'three-dimensional' micromachining via focused ion beam sputtering.

Acknowledgments

The authors thank Y.N. Picard, M.B. Ritchey (SNL), H. Apodaca (SNL) and A. Gunasekaran (LTU). MJV acknowledges support from the Louisiana Board of Regents. Part of this work was performed at Sandia National Laboratories and is supported by the United States Department of Energy under Contract No. DE-AC04–94AL85000. Sandia is a multiprogram laboratory operated by Sandia Corporation, a Lockheed Martin Company, for the United States Department of Energy.

References

[1] For a review of alternative microfabrication techniques, see Thornell G and Johansson S, Microprocessing at the Fingertips, J. Micromech. Microeng 1998;8:251–262.
[2] Masaki T, Kawata K, Masuzawa T. Micro Electro-Discharge Machining and its Applications. Proc IEEE MEMS 1990:21–6.
[3] Langen HH, Masuzawa T, Fujino M. Self-aligned machining and assembly of high aspect ratio microparts into silicon. Proc IEEE MEMS 1995:250–5.
[4] Vasile MJ, Friedrich CR, Kikkeri B, McElhannon R Micrometer-scale machining: tool fabrication and initial results. Precision Engineering, 1996;19(2/3):180–6.
[5] Yamagata Y, Mihara S, Nishioki N, Higuchi T. A new fabrication method for microactuators with piezoelectric thin films using precision cutting technique. Proc IEEE MEMS 1996:307–11.
[6] Takahata K, Shibaike N, Guckel H. A novel micro electro-discharge machining method using electrodes fabricated by the LIGA process. Proc IEEE MEMS 1999:238–43.
[7] Masuzawa T. Wire Electrodischarge grinding for micro machining. Annals of the CIRP 1985;34:431–4.
[8] See for example, Minitool, Inc., Los Gatos, CA, USA.
[9] Schaller Th, Bohn L, Mayer J, Schubert K. Microstructure grooves with a width of less than 50 μm cut with ground hard metal micro end mills. Precision Engineering 1999;23:229–35.
[10] Friedrich CR, Vasile MJ. Development of the micromilling process for high aspect ratio microstructures. J Microelectromech Sys 1996;5:33–8.
[11] Friedrich C, Coane P, Goettert J, Gopinathin N. Direct fabrication of deep x-ray lithography masks by micromechanical milling. Precision Engineering 1998;22:164–73.
[12] Masuzawa T, Fujino M. A process for manufacturing very fine pin tools. SME Tech. Papers 1990:MS90–307.
[13] Orloff J. High-resolution focused ion beams. Rev Sci Instrum 1993;64:1105–30.
[14] Ishitani T, Ohnishi T, Kawanami Y. Micromachining, and device transplantation using focused ion beam. Jap J Appl Phys 1990;29:2283–7.
[15] Vasile MJ, Biddick C, Schwalm SA. Microfabrication by ion milling: The lathe technique. J Vac Sci Technol B, 1994;12:2388.
[16] Russell PE, Stark TJ, Griffis DP, Phillips JR, Jarausch KF. Chemically, and geometrically enhanced focused ion-beam micromachining, J Vac Sci Technol B 1998;16:2494–8.
[17] Harriott LR. A second generation focused ion beam micromachining system. Proc SPIE 1987;190:773.
[18] The second apparatus was a joint project among Louisiana Tech University (IfM), the National Jet Company and Dover Instruments.
[19] Vasile MJ, Nassar R, Xie J, Guo H. Microfabrication techniques using focused ion beams and emergent applications. Micron 1999;30:235–44.
[20] Hardness values for the different metal alloy workpiece materials include 6061-T4 aluminum, Rockwell B =26; brass, Rockwell B = 35; 4340 steel, Rockwell B = 97.
[21] Vasile MJ, Nassar R, Niu Z, Zhang W, Liu S. Focused ion beam milling: depth control for three-dimensional microfabrication. J Vac Sci Technol B 1997;15:2350–4.